Polyhedron 239 (2023) 116431

Contents lists available at ScienceDirect

Polyhedron

journal homepage: www.elsevier.com/locate/poly

Copper(II)/diiminic complexes based on 2-hydroxybenzophenones: DNA- and BSA-binding studies and antitumor activity against HCT116 and HepG2 tumor cells

Júlia H.V. Rodrigues [a], Alexandre B. de Carvalho [a], Valdenizia R. Silva [b], Luciano de S. Santos [b], Milena B.P. Soares [a,c], Daniel P. Bezerra [b], Katia M. Oliveira [d], Rodrigo S. Corrêa [a,*]

[a] Departamento de Química, Instituto de Ciências Exatas e Biológicas—Campus Morro do Cruzeiro, Universidade Federal de Ouro Preto—UFOP, CEP 35400-000 Ouro Preto, MG, Brazil
[b] Instituto Gonçalo Moniz, Fundação Oswaldo Cruz (IGM-FIOCRUZ/BA), Salvador, Bahia 40296-710, Brazil
[c] Instituto SENAI de Inovação em Sistemas Avançados de Saúde, SENAI CIMATEC, Salvador, Bahia 41650-010, Brazil
[d] Instituto de Química, Universidade de Brasília (UnB) – Campus Darcy Ribeiro, Brasília – DF 70910-900, Brazil

ARTICLE INFO

Keywords:
Copper(II)
Diimines
2-Hydroxybenzophenones
Heteroleptic
DNA
BSA

ABSTRACT

Here, we report four new heteroleptic Cu(II) complexes with the formula [Cu(bipy)(2H4MeBz)]NO_3 (**1**), [Cu(phen)(2H4MeBz)]NO_3 (**2**), [Cu(bipy)(2H4OcBz)]NO_3 (**3**) and [Cu(phen)(2H4OcBz)]NO_3 (**4**), where the ligands are 2-hydroxy-4-methoxybenzophenone (2H4MeBz), 2-hydroxy-4-(octyloxy)benzophenone (2H4OcBz), 2,2′-bipiridine (bipy) and 1,10-phenantroline (phen). All compounds present two bidentate ligands, a monoanionic 2-hydroxybenzophenone, forming a six-membered chelate ring and the diiminic ring forming a five-membered chelate ring, as well as one nitrate as counterion located at the axial position, as suggested by the crystal structure of complex **2**. Complex/DNA interaction studies were also performed using spectroscopic titration (K_b close to 10^4 M^{-1}), viscosity, Hoechst 33258 competition, and circular dichroism, revealing a moderate interaction between them. Additionally, complexes **1**–**4** moderately interact with BSA (Bovine Serum Albumin). The compounds were evaluated against HCT116 (human colon carcinoma) and HepG2 (human hepatocellular carcinoma) cancer cells and against MRC-5 (human lung fibroblast), a noncancer cells. The cytotoxic results suggest that complexes **2** and **4** are more cytotoxic than **1** and **3**, showing that the presence of phen ligand may play an important role in increasing the biological effect of the compounds.

1. Introduction

Copper(II) complexes are promising metallodrug candidates focused on antitumor therapy [1–3], since cancer is one of the diseases that most afflict humanity in this century. Also, copper may be an alternative on platinum-based complexes, the main metallodrugs used in cancer treatment [4,5]. Thus, some copper advantages is the low cost, high accessibility, possibility of presenting many coordination numbers, structural and chemical diversity, and essential element to life [6]. Several copper complexes have shown efficacy in the treatment of many diseases, often being more active than their other transition metal analogs [7]. A strategy to obtain new active compounds can be to explore their interactions with DNA [8], trying to increase the specificity [9], and decrease the drug side effects [10].

According to Silva *et al.* 2011 [2], copper-based metal complexes can act as artificial nuclease, which can cause the DNA cleavage in hydrolytic or oxidative medium, in which is necessary to add an external reagent, such as a thyol and hydrogen peroxide. In the literature, there are many copper complexes with the ability to cleave DNA without external oxidative agent. These compounds present DNA binding constant (K_b) of approximately 10^4 M^{-1} [11]. Copper complexes can interact with DNA through other modes, such as intercalation, electrostatic interactions, or grooves [8,12]. In recent years, among the several active copper(II) complexes reported in the literature, we highlight Casiopein®, a promising anticancer [4,5], antimicrobial, antigiardiasis [13], and antichagas disease [14] class of compounds. Structurally, Casiopein® includes copper(II) complexes with general formula [CuL_1L_2]NO_3, where L_1 are primary ligands (referring to an aromatic diimine) and L_2

* Corresponding author.
E-mail address: rodrigocorrea@ufop.edu.br (R.S. Corrêa).

https://doi.org/10.1016/j.poly.2023.116431
Received 17 February 2023; Accepted 18 April 2023
Available online 21 April 2023

are secondary ligands, usually a bidentate ligand such as amino acids or β-diketones [4,15]. Several studies on this compoud class report the ability to cause cell death by apoptosis, producing reactive oxygen species that cause damage to DNA structures, preventing cell replication. Studies with Casiopeins® have proven a higher efficiency of these compounds in relation to platinum compounds, with a higher antiproliferative activity [4,5,13,15].

A ligand class that can be used to form Casiopeins®-like complexes is hydroxylated benzophenones. It is well known that benzophenone derivatives are notable for absorbing ultraviolet radiation in the UVB (λ = 290 to 320 nm) and UVA (λ = 320 to 360 nm) ranges and some UVC light (λ ≈ 250 to 290 nm) [16], through the excitation and transition of electrons from their fundamental state to their most excited state. Due to these characteristics of absorbing and dissipating UV radiation, benzophenones can be used in sunscreens [17,18]. Recently, 2-hydroxybenzophenones were used as ligand to obtain homoleptic copper(II)-based complexes in 2:1 ligand/metal ratio [19–23]. Here, we used two hydroxylated benzophenone derivatives known as 2-hydroxy-4-methoxybenzophenone (2H4MeBz) and 2-hydroxy-4-(ocilloxy)benzophenone (2H4OcBz) (Fig. 1) to obtain four heteroleptic copper(II) complexes with 2,2′-bipyridine(bipy)/1,10-phenantroline (phen) analogous to casiopein® structures. This class of complexes is the first examples of heteroleptic copper(II)-based complexes with 2-hydroxybenzophenones. The compounds were characterized, investigated regarding their BSA and DNA interactions, as well as cytotoxic activity against tumor cells (HCT116 and HepG2 cancer cells) and nontumor cells (MRC-5).

2. Experimental section

2.1. Materials and instruments

Copper(II) nitrate trihydrate, 2,2′-bipyridine (bipy), 1,10-phenanthroline (phen), 2–hydroxy-4-methoxybenzophenone (2H4MeBz), 2-hydroxy-4-(octyloxy)benzophenone (2H4OcBz), calf-thymus DNA (CT-DNA), and bovine serum albumin (BSA) were purchased from Sigma-Aldrich and used as received. Conductivity data (presented as S cm^2 mol^{-1}) were obtained in methanol, using an Instrutemp conductivity meter with a cell constant equal to 1.25 cm^{-1}. Measurements were made at room temperature (20 °C) using a 10 mM solution of the complex. Melting point measurements were acquired on a Fisatom model 431 D. Elemental analysis of the complex was carried out using a LECO Tru-Spec CHN analyzer. The electronic absorption spectra of all compounds were obtained in methanol solution using a Thermo Scientific Genesys 10 s UV–vis spectrophotometer. The room temperature (20 °C) ATR-FTIR spectrum was recorded on an FTIR spectrometer (ABB Bomen, model MB 3000) from 4000 to 500 cm^{-1}. The mass spectra were registered in methanol solution and acetonitrile: methanol (55:45, v/v) 50:50 as the mobile phase on an LCMS-IT-TOF mass spectrometer (Shimadzu).

2.2. General procedure to obtain Cu(II)/diiminic-2-hydroxybenzophenones complexes

For synthesis of complexes **1**–**4**, 0.25 mmol (0.570 g or 0.0815 g) of 2-hydroxyephenone (2H4MeBz or 2H4OcBz, respectively) and 0.03 mmol (5 mg) of KOH were added in 20 mL of methanol. This mixture was stirred for 5 min, and 0.25 mmol (0.060 g) of $Cu(NO_3)_2{\cdot}3H_2O$ was added and stirred for 20 min. Finally, 0.25 mmol (0.039 g or 0.045 g) of *N*-heterocyclic ligand (2,2′-bipiridine or 1,10-phenantroline, respectively) was added. The resulting solution was filtered of and kept under room temperature. Crystalline green solid was obtained by slow evaporation, washed with water and collected for characterization after one week.

(**1**) [Cu(bipy)(2H4MeBz)]NO_3: Yield 88%. Colour: green. Elemental analysis for ($CuC_{24}H_{19}N_3O_6$) calcd: C 56.64, H 3.76, N 8.26; found: C 56.81, H 3.68, N 8.43. M.p. = 254.9 °C (decomposition). ΛM (methanol) = 72 Ω^{-1} cm^2 mol^{-1}. HRMS ($CuC_{24}H_{19}N_2O_3$, $[M]^+$) calcd: 446.0709; found: 446.0703. ATR-FTIR (cm^{-1}): 3060, 2920, 1608, 1581, 1556, 1446, 1379, 1161, 750. UV–vis (methanol), λ^{max}/nm (ε/M $^{-1}cm^{-1}$) = 272 (36128); 381 (2590); 629 (59).

(**2**) [Cu(phen)(2H4MeBz)]NO_3: Yield 71%. Colour: green. Elemental analysis for ($CuC_{26}H_{19}N_3O_6$) calcd: C 58.59, H 3.59, N 7.88; found: C 58.55, H 3.60, N 7.96. M.p. = 256.4 °C (decomposition). ΛM (methanol) = 84 Ω^{-1} cm^2 mol^{-1}. HRMS ($CuC_{26}H_{19}N_2O_3$, $[M]^+$) calcd: 470.0692; found: 470.0702. ATR-FTIR (cm^{-1}): 1620, 1556, 1369, 1263, 1238, 1166, 757. UV–vis (methanol), λ^{max}/nm (ε/M $^{-1}cm^{-1}$) = 299 (37467); 376 (6867); 615 (11).

(**3**) [Cu(bipy)(2H4OcBz)]NO_3: Yield 90%. Colour: green. Elemental analysis for ($CuC_{31}H_{33}N_3O_6$) calcd: C 61.32, H 5.48, N 6.92; found: C 61.52, H 5.58, N 6.97. M.p. = 214.6 °C (decomposition). ΛM (methanol) = 92 Ω^{-1} cm^2 mol^{-1}. HRMS ($CuC_{31}H_{33}N_2O_3$, $[M]^+$) calcd: 568,1793; found: 568,1798. ATR-FTIR (cm^{-1}): 3473, 2921, 1600, 1579, 1556, 1444, 1379, 1245, 1166, 1116, 754. UV–vis (methanol), λ^{max}/nm (ε/M $^{-1}cm^{-1}$) = 299 (37467); 375 (6967); 614 (24).

(**4**) [Cu(phen)(2H4OcBz)]NO_3: Yield 81%. Colour: green. Elemental analysis for ($CuC_{33}H_{33}N_3O_6$) calcd: C 62.80, H 5.27, N 6.66; found: C

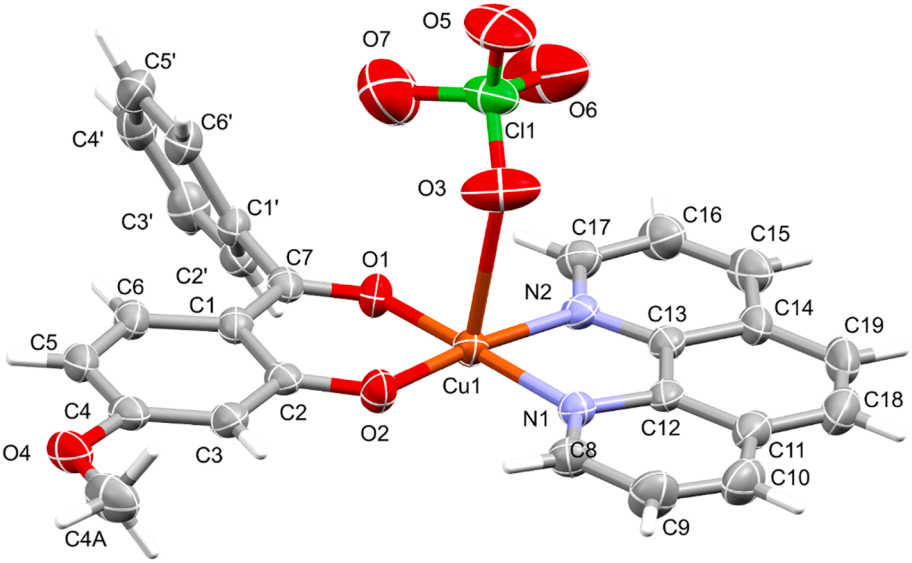

Fig. 1. Crystal structure of the complex [Cu(phen)(2H4MeBz)(ClO_4)] with ellipsoids at 30% of thermal probability and non-H atoms labelled.

61.99, H 5.65, N 6.94. M.p. = 213.1 °C (decomposition). ΛM (methanol) = 81 Ω^{-1} cm^2 mol^{-1}. HRMS ($CuC_{33}H_{33}N_2O_3$, $[M]^+$) calcd: 544.1789; found: 544.1798. ATR-FTIR (cm^{-1}): 3055, 2921, 1606, 1548, 1263, 1168, 1120, 752. UV–vis (methanol), λ^{max}/nm (ε/M $^{-1}cm^{-1}$) = 272 (19662); 324 (1546); 615 (28).

2.3. Single-crystal X-ray diffraction

The single crystal used in the X-ray experiment was obtained after recrystallization using different counterions, such as NH_4PF_6, NaCl and $NaClO_4$. For the exchange of the nitrate counterion by another counterion, a saturated methanolic solution was made from each of the salts (NH_4PF_6, NaCl or $NaClO_4$), and 5 mg of complex **2** was added to each system. Then, each solution was left at rest at room temperature to recrystallize the complexes, and the formed crystals were washed with water to eliminate the excess remaining salt. Quality crystals were obtained by using ClO_4^- contraction. Complex **2** was collected using an Agilent Super Nova diffractometer with graphite monochromatised MoKα radiation (λ = 0.71073 Å). The structure was solved by direct methods using the SHELXS-97 and refined through the model in F^2 using the SHELXL-97 program [24]. Mercury was used to analyze and elaborate graphical representations of structures [25]. Crystal parameters and details of data collection and refinement are shown in Table 1S.

2.4. Cytotoxic activity of complexes 1–4

The cytotoxicity activity of the complexes was investigated using the tumor cell lines HCT116 (human colon carcinoma) and HepG2 (human hepatocellular carcinoma) and the nontumor cell line MRC-5 (human lung fibroblast). The cells were cultured in Roswell Park Memorial Institute (RPMI 1640) medium supplemented with 10% fetal bovine serum (FBS). The cells were kept in incubators with an atmosphere of 5% CO_2 at 37 °C, and cell growth was monitored daily with the support of an inversion microscope. Cell cultures were negative for microplasm, as evaluated by Hoechst placement (Mycoplasma Stain Kit, Cat. MYC1, Sigma-Aldrich®, St Louis, MO, USA).

The cytotoxicity of the compounds was assessed by the alamar blue assay, which was performed after 72 h of treatment with the compounds. Initially, the cells were seeded in 96-well plates. After 24 h, compounds dissolved in DMSO were added to each well and incubated for 72 h. Doxorubicin was used as a positive control. The negative control received the same amount of DMSO. Four hours before the end of the incubation period, 20 μL of the stock solution (0.312 mg/mL) of alamar blue (resazurin) was added to each well. The absorbances were measured at wavelengths of 570 nm (reduced) and 595 nm (oxidized) using a plate reader [26]. The percentage of inhibition was calculated, and the percentage of inhibition × log of the concentration was recorded. The IC_{50} was determined from nonlinear regression using the Prisma version 5.0 program (GraphPad Software).

2.5. Complex/DNA interaction studies

DNA solution was prepared by diluting 2 mg of CT-DNA (Calf-thymus DNA) in 1 mL of Tris-HCl buffer (4.5 mM Tris-HCl, 0.5 mM Tris-base, and 50 mM NaCl, pH = 7.4). The CT-DNA concentration was calculated using the molar extinction coefficient at 260 nm (ε = 6600 $M^{-1}cm^{-1}$).

Spectroscopic titration were performed using a solution of complexes prepared in Tris-HCl buffer containing 10% DMSO. Successive additions of CT-DNA aliquots were added to cuvettes containing the complex, and after solution equilibration for approximately 1 min, the spectra were recorded. At each addition, correction of CT-DNA absorption was performed. The absorption intensity with increasing concentrations of CT-DNA was analyzed, and the binding constant (K_b) between the complex and DNA was calculated by the following Equation (1) [27]:

$$\frac{[DNA]}{\varepsilon_a - \varepsilon_b} = \frac{[DNA]}{\varepsilon_b - \varepsilon_f} + \frac{1}{K_b\,(\varepsilon_b - \varepsilon_f)} \quad (1)$$

where [DNA] is the concentration of CT-DNA, εa is the extinction coefficient corresponding to the Aobs/[complex], εf is the extinction coefficient of the free complex and εb is the extinction coefficient of the DNA-bound complex. The intercept of [DNA]/(εa – εb) versus [DNA] originates on a line whose inclination and intercept are 1/(εb – εf) and 1/K_b (εb – εf), respectively. Thus, K_b was extracted from the ratio between the angular coefficient (slope) and the linear coefficient (intercept).

Viscosity measurements. The viscosity experiments were performed using an Oswald viscosimeter in a thermostatic bath at 37 °C. Solutions were prepared keeping the CT-DNA concentration constant at 50 μM and varying the concentrations of copper complexes (5 to 30 μM) to obtain different molar ratios of [copper complex]/[CT-DNA]. The percent DMSO was kept constant at 10%. The samples were incubated for 18 h at 37 °C, and then, a digital stopwatch was used to measure the solution flow times in triplicate. The results were analyzed using a graph of relative viscosity $(\eta/\eta 0)^{1/3}$ vs ([complex]/[DNA]), where a η and η0 are the viscosities of CT-DNA in the presence and absence of the copper complexes, respectively. η and η0 were obtained using the relation $(t - t_{DNA})/t_{DNA}$, where t is the observed flow time of DNA in the presence of complexes and t_{DNA} is the flow time of the DNA in the absence of complexes.

Circular dichroism (CD). The CD experiment was carried out using a Jasco J-720 spectropolarimeter and a circular quartz cuvette with an optical path of 1 cm in the region of 240 to 350 nm at a speed of 200 nm/min, with 3 accumulations at each measurement and a constant nitrogen flow. CT-DNA solutions (50 μM) were prepared in the absence and presence of the copper complexes in different molar ratios ([complex]/[CT-DNA]): 0.1 to 0.5) and were incubated at 37 °C for 18 h. Then, the samples were analyzed.

Competitive assay. The competition assay was performed using Hoechst 33258 as a fluorescent probe by monitoring the fluorescence suppression of the CT-DNA-Hoechst system. Solutions containing CT-DNA (125 μM) and Hoechst 33258 (2.5 μM) were prepared, and then, copper complexes were added at different concentrations to obtain different molar ratios in Tris-HCl buffer (10% DMSO). Then, 200 μL of each solution was added to the wells of an opaque 96-well plate in triplicate. The fluorescence was analyzed using a SpectraMax i3 fluorimeter by exciting at 343 nm and acquiring the spectra in the range of 300 to 500 nm.

Table 1
Cytotoxic activity of complexes **1**–**4** and oxaliplatin (OXA) (IC_{50} in μM and their respective 95%CI) compared to tumor and nontumor cell lines.

Complexes	HCT116	HepG2	MRC-5	IS^1	IS^2
1	64.09 (47.05–87.31)	36.66 (30.47–44.11)	50.22 (38.47–65.56)	1.36	0.77
2	5.46 (4.63–6.42)	3.28 (2.93–3.68)	4.65 (4.00–5.42)	1.42	0.85
3	39.36 (28.18–54.98)	> 41.17	> 41.17	>1.00	>1.04
4	5.32 (4.63–6.13)	5.75 (5.13–6.43)	5.26 (4.91–5.64)	0.91	0.98
OXA	4.10(2.30–5.50)	2.20(1.30–3.80)	1.30(1.00–2.20)	0.58	0.31

HCT116 = human colon carcinoma, HepG2 = human hepatocellular carcinoma and MRC-5 = human lung fibroblast.
IS^1 = Selectivity index IC_{50} MRC-5/IC_{50} HepG2 and IS^2 = Selectivity index IC_{50} MRC-5/IC_{50} HCT116.

2.6. BSA interaction studies – Spectrofluorometric titration

The interaction between copper(II) complexes and BSA was performed by measuring the fluorescence suppression of tryptophan residues of this protein (spectrofluorimetric titrations). BSA (2.5 μM) solution was prepared by dissolving the protein in Tris-HCl buffer at pH 7.4. The complexes at different concentrations were added to the BSA solution to obtain different molar ratios ([complex]/[BSA]). The BSA concentration was kept constant in all samples. Then, 200 μL of the final solution was added to the 96-well opaque plate, and the quenching of the emission intensity of BSA at 340 nm (λexcitation 280 nm) was monitored at 298 and 310 K, using a SpectraMax M3 fluorimeter. The quantitative analysis of the BSA fluorescence suppression process was performed using the Stern-Volmer equation (5):

$$\frac{F_0}{F} = 1 + K_{sv}\,[Q] = 1 + k_q t_0\,[Q] \quad (2)$$

where F0 and F are the fluorescence intensities in the absence and presence of the complexes, respectively [Q] is the concentration of the copper(II) complexes (quenchers), Ksv is the Stern-Volmer constant, kq is the biomolecular quenching rate constant, and τ0 is the average lifetime of fluorescence of BSA in the absence of the complexes. The Ksv constant was obtained by linear regression of the plot of F0/F versus [Q], and kq was obtained by the ratio between Ksv and τ_0 [28].

To determine the ΔH°, ΔS° and ΔG° parameters, the following equations were used:

$$\ln\left(\frac{K_{b1}}{K_{b2}}\right) = \left(\frac{1}{T_1} - \frac{1}{T_2}\right) \times \frac{\Delta H^\circ}{R} \quad (3)$$

$\Delta G^\circ = -RT\ln K_b = \Delta H^\circ - T\Delta S^\circ$.

where K_{b1} and K_{b2} are the binding constants at temperatures T1 (298 K) and T2 (310 K), respectively, R is the universal constant of gases (8.314 J.mol^{-1}. K^{-1}), ΔH° is the enthalpy value, ΔS° is the entropy value and ΔG° is the Gibbs free energy of the o system.

3. Results and discussion

3.1. Synthesis and characterization

Complexes **1**–**4** were obtained from the reaction of $Cu(NO_3)_2{\cdot}3H_2O$ with ligands 2,2′-bipyridine (bipy), 1,10-phenanthroline (phen), 2–hydroxy-4-methoxybenzophenone (2H4MeBz) and 2-hydroxy-4-(octyloxy)benzophenone (2H4OcBz) in methanol, as described in Scheme 1. The proposed formula for the compounds are [Cu(bipy)(2H4MeBz)]NO_3 (**1**), [Cu(phen)(2H4MeBz)]NO_3 (**2**), [Cu(bipy)(2H4OcBz)]NO_3 (**3**) and [Cu(phen)(2H4OcBz)]NO_3 (**4**).

The copper(II) complexes were obtained as air-stable green solids, with crystalline appearance and with satisfactory yield (70 to 90%). The molar conductivity values for all complexes in methanol indicated that 1–4 are 1:1 electrolytes [29], with NO_3^- acting as a counterion in solution. In addition, elemental analysis (% of C, H and N) of complexes **1**–**4** is in agreement with the proposed structures. The UV–vis spectra for complexes **1**–**4** showed a band with maximum absorption in the region from 272 to 299 nm, referring to π → π* transitions, assigned to intra-ligand transitions (IL). The bands in the region between 376 and 381 nm can be attributed to metal–ligand charge transfer (MLCT). Finally, bands between 615 and 629 nm are attributed to d-d transitions that occur between copper(II) d-orbitals.

The FT-IR spectra of complexes showed bands in the region of 3148 cm^{-1} and 3383 cm^{-1} due to aromatic C—H groups of the benzophenones, 2,2′-bipyridine, or 1,10′-phenanthroline ligands. The 2-hydroxybenzophenones free present band at approximately 3400 cm^{-1}, which is related to the O—H hydroxyl stretching vibration. However, this band is not present in the four complex spectra, indicating OH group deprotonation. The C═O stretching vibrations observed at 1634 cm^{-1} and 1629 cm^{-1} for the ligands free 2H4MeBz and 2H4OcBz, respectively, shift to lower wavenumber close to 1600 cm^{-1}. The nitrate group presents two bands, which may indicate coordination to the metallic center, in solid. These bands are observed in the regions from 767 to 796 cm^{-1} and from 1369 to 1386 cm^{-1}, which are references to the stretching ν(ONO) and to the deformation of the structure in δ(ONO), respectively. Also, several attempts to obtain well-shaped single crystals for **1**–**4** were carried out.

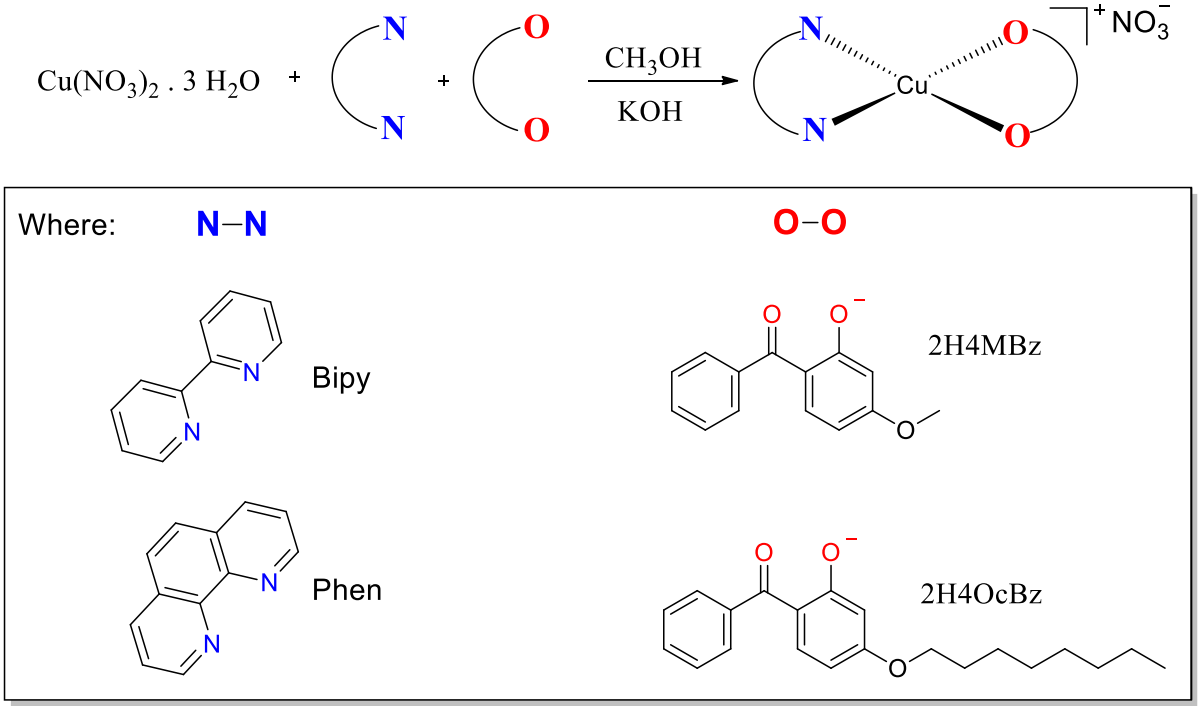

Scheme 1. General synthetic route used to obtain the copper(II) complexes (**1** – **4**).

However, using the compounds ([Cu(N—N)(L)]NO_3) that present nitrate as a counterion, only twinned or small crystals were obtained. Thus, one strategy was to exchange the NO_3^- counterion for ClO_4^-. Well-shaped single crystals were formed for complex **2** and ClO_4^-. The single crystal was analyzed by single crystal X-ray diffraction, resulting in the complex [Cu(phen)(2H4MeBz)(ClO_4)] (Fig. 1).

The crystal structure of the complex [Cu(phen)(2H4MeBz)(ClO_4)] confirmed the bidentate coordination of the *N*-heterocyclic (phen) and 2-hydroxybenzophenone (2H4MeBz) ligands to the copper(II). The structure of the [Cu(phen)(2H4MeBz)]ClO_4 complex presents a distorted square pyramidal geometry with a coordination number of five. The angle between copper(II) and the two nitrogen atoms (N1-Cu1-N2) of the phenanthroline ligand is close to 90°, while the O1-Cu1-O2 bond angle is slightly>90°. The torsion angle between copper(II) and phenanthroline is −0.34°. A value close to zero indicates that the phen ligand is coplanar to copper(II). The distance of the C7 = O1 double bond of 2H4MeBz in the complex is 1.275(6) Å, while in the free ligand, the value is 1.255 Å, increasing this bond by coordination. On the other hand, the *C*2-O2 single bond in the coordinated ligand is 1.319(7) Å and 1.355 Å in the free ligand [30], shortening of this bond. This aspect indicates electron delocalization in this structural moiety. The complex presents a phenanthroline ligand that forms a five-member quelate ring and a 2H4MeBz ligand forming a six-membered quelate ring. At the equatorial position, a perchlorate ion is coordinated as monodentate. The large bond length Cu1-O3 [2.507(6) Å] compared with bond lengths Cu1-O1 [1.903(4) Å] and Cu1-O2 [1.867(4) Å] indicate that the axial ligand is weakly coordinated to copper(II), justifying the ion labilization in solution, forming a 1:1 electrolyte. The larger bond length at the equatorial position compared with the other bonds is common for Cu(II) complexes, [31] due to the Jahn-Teller effect.

3.2. Cytotoxicity of complexes 1–4

The cytotoxic activity of complexes **1**–**4** was investigated against two tumor cell lines, namely, HCT116 (human colon carcinoma) and HepG2 (human hepatocellular carcinoma), and against a nontumor cell line, MRC-5 (human lung fibroblast), using the Alamar blue test [26]. IC_{50} (concentration that inhibits 50% of cell growth) values were determined for each complex after 72 h of cell exposition at different concentrations. The cytotoxic activity of oxaliplatin (OXA) [32] was used for comparison purposes. The IC_{50} results are presented in Table 1.

Firstly, the cytotoxic activity of the free ligands (2H4MeBz, 2H4OcBz, bipy and phen) was investigated and they were not cytotoxic at 100 μM, the highest concentration studied. All complexes are cytotoxic against tumor cells; however, complexes **2** and **4**, containing the 1,10-phenantroline ligand, were the most active complexes compared to complexes **1** and **3**, containing 2,2′-bipyridine. These results are consistent with recent reports that showed that the cytotoxic activity of complexes containing phenanthroline is higher than that of Cu(II) bipyridine complexes [14]. Phenanthroline planarity can likely provide a more effective interaction with DNA target. Also, these results also demonstrate the importance of ligand lipophilicity in the design of new complexes. Slight variations in structure can affect the cytotoxicity of the complexes. The presence of phenanthroline can increase the lipophilicity of the complex and facilitate its uptake by cells, consequently, making complexes with this ligand more cytotoxic.

Complex **2** was more cytotoxic against the HepG2 tumor cell line than complexes **1**, **3** and **4**. Comparing the IC_{50} values of copper(II) complexes and oxaliplatin, it is observed that the copper(II) complexes present lower IC_{50} values than oxaliplatin against all cell lines studied, especially complexes **2** and **4**, making these complexes promising. Additionally, copper(II) complexes showed higher selectivity against tumor cells than oxaliplatin. To better understand the mechanism of action of the compounds, interactions between complexes **1**–**4** with macromolecules, such as DNA and BSA, were performed.

3.3. Interaction with CT-DNA

The interaction between copper(II) complexes (**1** – **4**) and DNA was investigated as a useful tool to understand the main types of interactions, such as DNA intercalation, electrostatic or minor/major groove interactions. To determine the mode of interaction, spectroscopic titrations were carried out to obtain the intrinsic complex/CT-DNA binding constants (K_b). The successive additions of CT-DNA caused a decrease in the value of the absorption bands (hypochromism), while the λ^{max} value remained constant (Fig. 2). The K_b values were obtained using the equation [DNA]/(εa-εf) × [DNA]. The values found were 2.60 × 10^4 M^{-1} for complex **1**, 5.37 × 10^4 M^{-1} for complex **2**, 2.42 × 10^4 M^{-1} for complex **3** and 1.98 × 10^4 M^{-1} for complex **4**. These results are close to that one found for copper(II)/5,5′-dimethyl-2,2′-bipyridine-based complex recently reported[33]. In addition, these values are similar to other ternary copper(II) complexes reported in the literature[34,35], but smaller values than the K_b value for DNA-intercalator complexes[36], indicating that the complexes **1**–**4** can interact weakly with DNA, through electrostatic interactions or via grooves, in which complex **2** presented high DNA affinity than the other three complexes.

Viscosity studies were conducted to obtain more information about the interaction between complexes and CT-DNA. For comparison, the orange thiazole compound, a known DNA intercalator, was used[36,37]. Therefore, orange thiazole caused an increase in the relative viscosity of CT-DNA with increasing concentration due to base pair separation. Electrostatic or groove interactions do not change viscosity significantly, but covalent interactions cause a decrease in viscosity values by shortening its length [38]. Fig. 2 presents the viscosity of CT-DNA in the presence of copper(II) complexes **1**–**4**, and none of the complexes caused significant alterations in the DNA viscosity. Thus, electrostatic or minor grooves may be the possible modes of interactions.

Circular dichroism is a useful and sensitive technique to analyze changes in DNA structure caused by interactions with metal complexes. For this, the CT-DNA spectrum was monitored in the presence of different concentrations of copper(II) complexes (Ri = [complex]/[CT-DNA] = 0.1 to 0.5). The CT-DNA spectrum exhibits a positive band at 275 nm due to base stacking and a negative band at 245 nm due to right-handed helicity, as shown in Fig. 2. The results showed that the complexes did not change the DNA structure, since the CT-DNA bands did not undergo significant change.

A competitive binding assay with Hoechst 33258, a fluorescent dye that interacts with DNA through the minor groove, was performed [39]. When excited at 340 nm, Hoechst 33258 in the presence of CT-DNA emitted fluorescence at 370 nm. Compounds that bind to DNA by minor grooves can replace Hoechst of the CT-DNA structure, and consequently, there is a decrease in the intensity of fluorescence. In the presence of copper(II) complexes, a substantial decrease in the Hoechst-DNA fluorescence intensity was observed, which indicates that the complexes can interact with CT-DNA via minor grooves.

In view of the results, it can be inferred that the copper(II) complexes probably interact with CT-DNA via minor grooves and electrostatic interactions, given the positive charge of the complexes and the negative charge of the CT-DNA.

3.4. Interaction studies with BSA

Serum albumin is the most abundant plasma protein and is responsible for transporting various types of metabolites, drugs, nutrients and other molecules [40]. Thus, it is important to understand the interaction between new complexes with chemotherapeutic potentials and albumin, since this protein binds and delivers the compounds through the body.

Due to these characteristics, serum albumin, more precisely bovine serum albumin (BSA), is one of the most studied proteins due to its structural similarity with human serum albumin. BSA emits fluorescence; however, when it binds to a metal complex, the fluorescence intensity of the BSA- complex is altered.

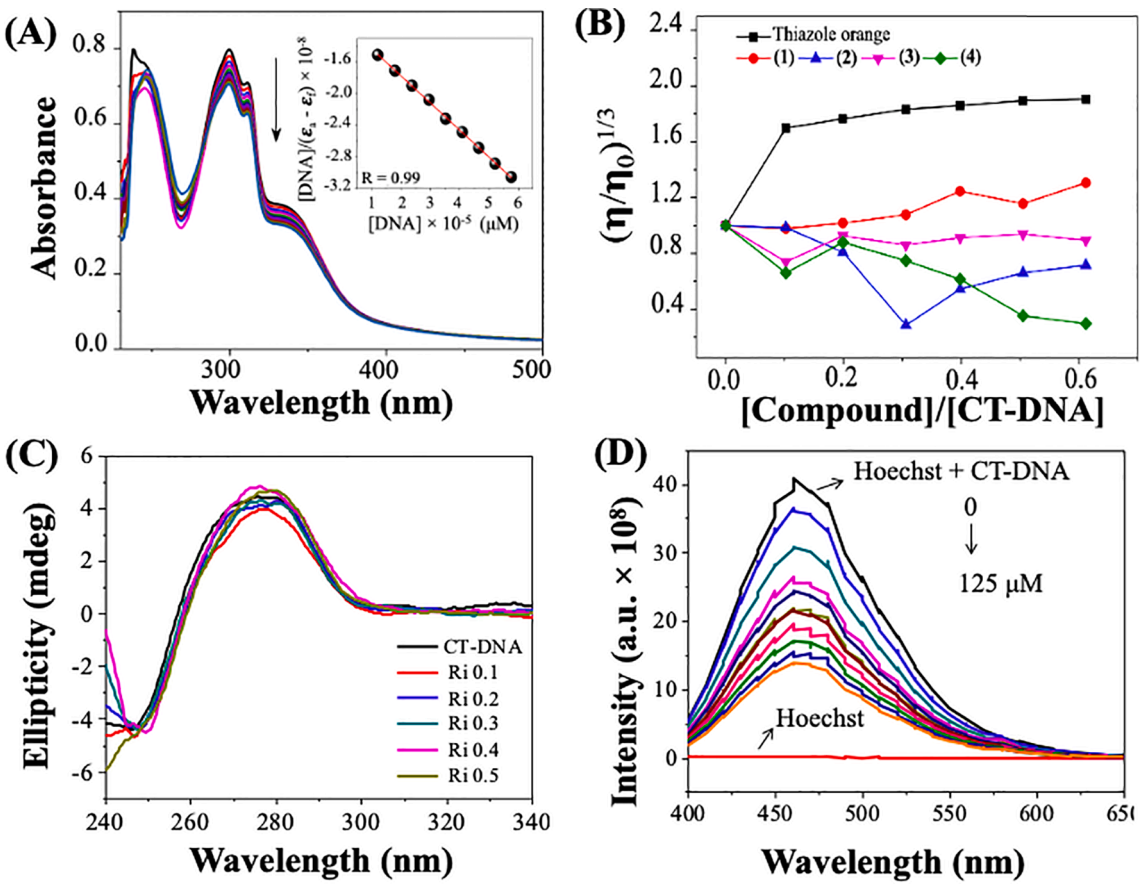

Fig. 2. (**A**) Electronic absorption spectra of complex (**3**) at a concentration of 5×10^5 mol/L in the presence of increasing concentrations of CT-DNA solution and [DNA]/(εa-εf) vs [DNA]. (**B**) Effect of increasing amounts of complexes 1–4 and thiazole orange on the viscosity of CT-DNA (50 μM) in Tris-HCl buffer (pH = 7.4) (**C**) Circular dichroism spectra of CT-DNA (50 μM) in the presence of different concentrations of complex 4 in Tris-HCl buffer (pH 7.4). (**D**) Fluorescence quenching of Hoechst 33258-CT-DNA (λex = 343 nm) solution in the absence and presence of different concentrations of complex **4** (0–125 μM).

The fluorescence emission spectra of BSA in the absence and presence of copper(II) complexes were registered at 298 and 310 K. As shown in Fig. 3, the fluorescence intensity decreased considerably with increasing concentrations of the complexes, indicating interactions between copper(II) complexes and the protein. The interaction can occur by two mechanisms, dynamic and static. In the dynamic mechanism, the fluorophore comes in contact with the quencher (copper complexes) in the excited state, and in the static mechanism, the interaction occurs in the ground state [28]. The dynamic mechanism is favoured with increasing temperature since there is an increase in the diffusion coefficient. However, at higher temperatures, the stability of the complexes formed between the fluorophore and quencher decreased in a static mechanism. Thus, the dynamic and static mechanisms can be distinguished by analyzing the Stern-Volmer constant (K_{sv}) values at different temperatures.

After the spectrofluorimetric titrations used to study the mode of interaction that occurs between the synthesized copper(II) complexes and BSA and using the Stern-Volmer equation (3), the values of constants for each of the compounds were obtained. Additionally, through equations 6 and 7, it was possible to determine the ΔH°, ΔS° and ΔG° values for the four copper(II) complexes, where they can be seen in Table 2.

It is noted that for complexes **1**, **3** and **4**, there was an increase in the K_{sv} constant along with the increase in temperature, which indicates a dynamic mechanism. However, complex **2** had a constant value of K_{sv} that decreased with increasing temperature, which may indicate a static mechanism. It can be affirmed that the mode of interaction between the complexes and BSA was spontaneous at the two temperatures analyzed because the Gibbs energy values were negative ($\Delta G < 0$). For the other parameters, complex 1 presented both negative ΔH and ΔS values, corresponding to van der Waals forces and interactions by hydrogen bonds; complexes **2** and **3** had positive ΔH and ΔS values, which indicate the involvement of hydrophobic interactions between the complexes and BSA; finally, for complex **4**, there was a negative value for ΔH and a positive value for ΔS, which indicates that an electrostatic interaction occurs [2,41,42].

An interesting fact observed is that complex **4** presented the highest K_b value compared to the others, indicating a stronger interaction with BSA. Similar results are found in the literature [37]. This complex also presented a high interaction with DNA. In view of that, we can assume that albumin acts as a carrier of this complex until it reaches a point in the body where it will release to act by inhibiting cell proliferation. The same cannot be said for the other complexes, whose K_b values were lower. The number of sites (n) were close to 1, indicating that all complexes interact with only one BSA site.

4. Conclusion

In summary, four new ternary copper(II) complexes with 2-hydroxy-4-ocillobenzophenone (2H4OcBz) and 2H4MeBz (2H4MeBz) and *N*-heterocyclic ligands (1,10-phenanthroline and 2,2′-bipyridine) were synthesized and characterized. The complexes with formula [Cu(bipy)(2H4MeBz)]NO_3 (**1**), [Cu(phen)(2H4MeBz)]NO_3 (**2**), [Cu(bipy)(2H4OcBz)]NO_3 (**3**) and [Cu(phen)(2H4OcBz)]NO_3 (**4**) present two bidentate ligands at the equatorial position. The complexes interact moderately with DNA, presenting K_b values in the range of 1.98×10^4 to

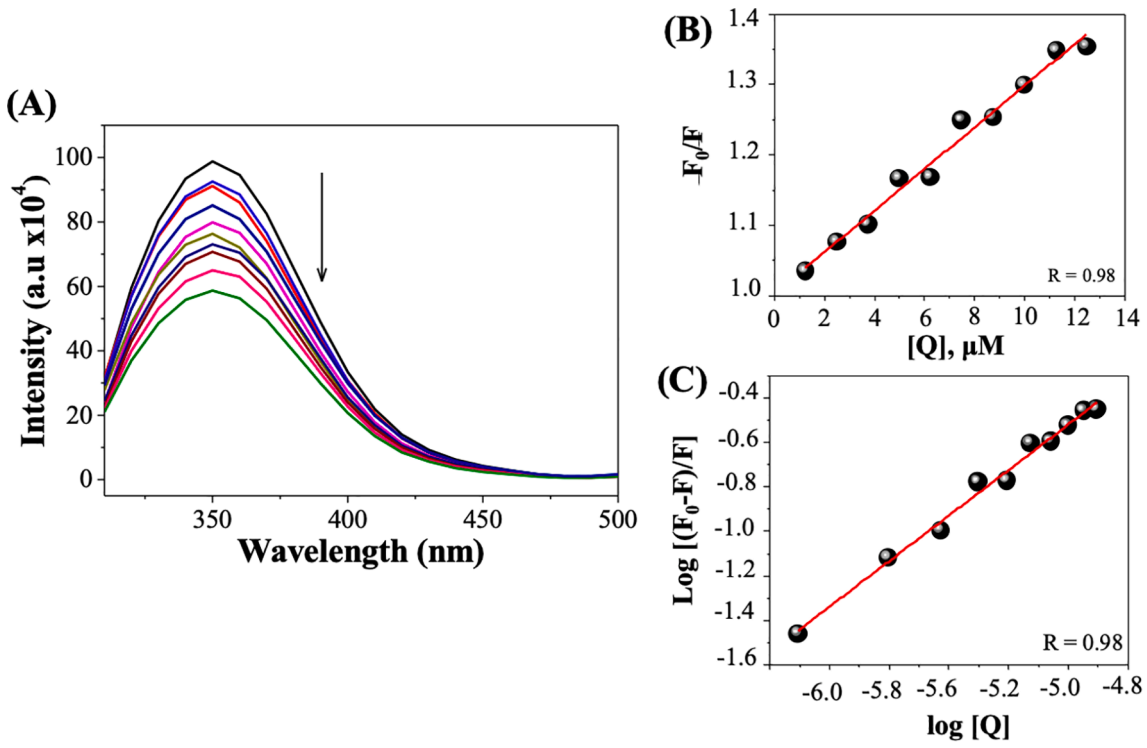

Fig. 3. (**A**) Fluorescence emission spectra of BSA (2.5 μM; λex = 280 nm; λem = 340 nm, at 298 K) in the absence and presence of increasing concentrations of complex 4 (0 – 50 μM). (**B**) Plot of F0/F vs [Q] and (**C**) plot of log[(F0-F)/F] vs log [Q].

Table 2
Interaction parameters of copper(II) complexes synthesized with BSA at temperatures of 298 and 310 K.

	T(K)	K_{sv} / (M^{-1})	k_q (M^{-1} s^{-1})	K_b (M^{-1})	*n*	ΔH° (kJ/mol)	ΔG° (kJ/mol)	ΔS° (J/K mol^{-1})
1	298	$(6.89 \pm 0.06) \times 10^4$	6.89×10^{13}	$(1.30 \pm 0.03) \times 10^4$	0.85	−29.77	−23.46	−21.15
	310	$(7.71 \pm 0.10) \times 10^4$	7.71×10^{13}	$(2.07 \pm 0.75) \times 10^4$	0.66		−25.61	−13.42
2	298	$(5.01 \pm 0.09) \times 10^4$	5.01×10^{13}	$(6.88 \pm 0.27) \times 10^4$	1.04	46.25	−27.59	247.81
	310	$(2.85 \pm 0.11) \times 10^4$	2.85×10^{13}	$(3.34 \pm 0.87) \times 10^4$	1.01		−26.37	235.80
3	298	$(8.38 \pm 0.36) \times 10^4$	8.38×10^{13}	$(2.12 \pm 0.15) \times 10^3$	0.65	20.04	−18.97	130.93
	310	$(9.44 \pm 0.13) \times 10^4$	9.44×10^{13}	$(1.55 \pm 0.03) \times 10^3$	0.61		−18.93	125.73
4	298	$(6.43 \pm 0.55) \times 10^4$	6.43×10^{13}	$(3.31 \pm 0.11) \times 10^5$	1.14	−27.16	−31.48	14.51
	310	$(7.58 \pm 0.80) \times 10^4$	7.58×10^{13}	$(5.06 \pm 0.79) \times 10^5$	0.96		−33.85	21.57

5.37×10^4 M^{-1}. Also, complex/BSA interaction studies were carried out, indicating that complex **1** presents van der Waals interactions or hydrogen bonds, while complexes **2** and **3** present hydrophobic interactions, and complex **4** interacts by electrostatic forces. The cytotoxic assays against HCT116 and HepG2 tumor cells indicated that complexes **2** and **4** present lower IC_{50} values and higher selectivity for distinct tumor cells. Thus, complexes containing 2-hydroxybenzophenone and 1,10-phenanthroline were the most promising ones and can be further investigated as antitumor drugs.

CRediT authorship contribution statement

Júlia H.V. Rodrigues: Conceptualization, Data curation, Formal analysis, Investigation, Methodology, Resources, Software, Validation, Visualization, Writing – original draft. **Alexandre B. de Carvalho:** Conceptualization, Data curation, Formal analysis, Investigation, Methodology, Resources, Software, Validation, Visualization, Writing – original draft. **Valdenizia R. Silva:** Data curation, Formal analysis, Investigation, Methodology. **Luciano de S. Santos:** Data curation, Formal analysis, Investigation, Methodology. **Milena B.P. Soares:** Funding acquisition, Supervision. **Daniel P. Bezerra:** Formal analysis, Funding acquisition, Writing – review & editing, Supervision. **Katia M. Oliveira:** Conceptualization, Formal analysis, Writing – review & editing, Supervision. **Rodrigo S. Corrêa:** Funding acquisition, Software, Validation, Visualization, Writing – review & editing, Supervision.

Declaration of Competing Interest

The authors declare that they have no known competing financial interests or personal relationships that could have appeared to influence the work reported in this paper.

Data availability

Data will be made available on request.

Acknowledgments

The authors are grateful for the financial support provided by the Brazilian Agencies of Research: FAPEMIG, CAPES and CNPq. J.H.V. Rodrigues thanks UFOP for master's fellowship. R. S. Correa would like to thank CNPq (311302/2020-3) and FAPEMIG (APQ-01674-18). The authors would like to thank Ananda Lima Sanson (UFOP) for the excellent mass spectrometry service. Authors also thank professors A.C.

Doriguetto form UNIFAL-MG for provide us the 2H4OcBz ligand and C. C. Corrêa form UFJF for X-ray diffraction facilities.

Appendix A. Supplementary data

Supplementary data to this article can be found online at https://doi.org/10.1016/j.poly.2023.116431.

References

[1] K. Gałczyńska, Z. Drulis-Kawa, M. Arabski, Antitumor activity of Pt(II), Ru(III) and Cu(II) complexes, Molecules 25 (2020), https://doi.org/10.3390/molecules25153492.

[2] P.P. Silva, W. Guerra, J.N. Silveira, A.M. da C. Ferreira, T. Bortolotto, F.L. Fischer, H. Terenzi, A. Neves, E.C. Pereira-Maia, Two new ternary complexes of copper(II) with tetracycline or doxycycline and 1,10-phenanthroline and their potential as antitumoral: cytotoxicity and DNA cleavage, Inorg. Chem. 50 (2011) 6414–6424, https://doi.org/10.1021/ic101791r.

[3] P.S. Lopes, D.A. Paixão, F.C.S. de Paula, A.M.D.C. Ferreira, J. Ellena, S. Guilardi, E. C. Pereira-Maia, W. Guerra, A new copper(II) complex with 2-thenoyltrifluoroacetone and 2,2-bipyridine: Crystal structure, spectral properties and cytotoxic activity, J. Mol. Struct. 1034 (2013) 84–88, https://doi.org/10.1016/j.molstruc.2012.09.022.

[4] J.R. Valdez-Camacho, Y. Pérez-Salgado, A. Espinoza-Guillén, V. Gómez-Vidales, C. Alberto Tavira-Montalvan, A. Meneses-Acosta, M.A. Leyva, M.G. Vázquez-Ríos, E. Juaristi, H. Höpfl, L. Ruiz-Azuara, J. Escalante, Synthesis, structural characterization and antiproliferative activity on MCF-7 and A549 tumor cell lines of [Cu(N-N)(β3-aminoacidate)]NO3 complexes (Casiopeínas®), Inorganica Chim Acta. 506 (2020), 119542, https://doi.org/10.1016/j.ica.2020.119542.

[5] J.C. García-Ramos, A.G. Gutiérrez, A. Vázquez-Aguirre, Y. Toledano-Magaña, A. L. Alonso-Sáenz, V. Gómez-Vidales, M. Flores-Alamo, C. Mejía, L. Ruiz-Azuara, The mitochondrial apoptotic pathway is induced by Cu(II) antineoplastic compounds (Casiopeínas®) in SK-N-SH neuroblastoma cells after short exposure times, Biometals 30 (2017) 43–58, https://doi.org/10.1007/s10534-016-9983-8.

[6] E. Meggers, Exploring biologically relevant chemical space with metal complexes, Curr. Opin. Chem. Biol. 11 (2007) 287–292, https://doi.org/10.1016/j.cbpa.2007.05.013.

[7] M. Baldini, M. Belicchi-Ferrari, F. Bisceglie, G. Pelosi, S. Pinelli, P. Tarasconi, Cu(II) complexes with heterocyclic substituted thiosemicarbazones: The case of 5-formyluracil. Synthesis, characterization, X-ray structures, DNA interaction studies, and biological activity, Inorg. Chem. 42 (2003) 2049–2055, https://doi.org/10.1021/ic026131d.

[8] B.J. Pages, D.L. Ang, E.P. Wright, J.R. Aldrich-Wright, Metal complex interactions with DNA, Dalton Trans. 44 (2015) 3505–3526, https://doi.org/10.1039/C4DT02700K.

[9] R. Galindo-Murillo, J.C. García-Ramos, L. Ruiz-Azuara, T.E. Cheatham III, F. Cortés-Guzmán, Intercalation processes of copper complexes in DNA, Nucleic Acids Res. 43 (2015) 5364–5376, https://doi.org/10.1093/nar/gkv467.

[10] F.T. Martins, J.W. Cruz, P.B.M.C. Derogis, M.H. Dos Santos, M.P. Veloso, J. Ellena, A.C. Doriguetto, Natural polyprenylated benzophenones: Keto-enol tautomerism and stereochemistry, J. Braz. Chem. Soc. 18 (2007) 1515–1523, https://doi.org/10.1590/S0103-50532007000800011.

[11] S.S. Bhat, A.A. Kumbhar, H. Heptullah, A.A. Khan, V.V. Gobre, S.P. Gejji, V. G. Puranik, Synthesis, electronic structure, DNA and protein binding, DNA cleavage, and anticancer activity of fluorophore-labeled copper(II) complexes, Inorg. Chem. 50 (2011) 545–558, https://doi.org/10.1021/ic101534n.

[12] J.C. García-ramos, R. Galindo-murillo, F. Cortés-guzmán, L. Ruiz-azuara, C. Conjunto, D. Investigación, Q. Sustentable, Metal-based drug-DNA interactions, J. Mex. Chem. Soc. 57 (2013) 245–259.

[13] Y. Rufino-González, M. Ponce-Macotela, J.C. García-Ramos, M.N. Martínez-Gordillo, R. Galindo-Murillo, A. González-Maciel, R. Reynoso-Robles, A. Tovar-Tovar, M. Flores-Alamo, Y. Toledano-Magaña, L. Ruiz-Azuara, Antigiardiasic activity of Cu(II) coordination compounds: Redox imbalance and membrane damage after a short exposure time, J. Inorg. Biochem. 195 (2019) 83–90, https://doi.org/10.1016/j.jinorgbio.2019.03.012.

[14] D.A. Paixão, I.M. Marzano, E.H.L. Jaimes, M. Pivatto, D.L. Campos, F.R. Pavan, V. M. Deflon, P.I. da S. Maia, A.M. Da Costa Ferreira, I.A. Uehara, M.J.B. Silva, F. V. Botelho, E.C. Pereira-Maia, S. Guilardi, W. Guerra, Novel copper(II) complexes with hydrazides and heterocyclic bases: Synthesis, structure and biological studies, J. Inorg. Biochem. 172 (2017) 138–146, https://doi.org/10.1016/j.jinorgbio.2017.04.024.

[15] A.G. Gutiérrez, A. Vázquez-Aguirre, J.C. García-Ramos, M. Flores-Alamo, E. Hernández-Lemus, L. Ruiz-Azuara, C. Mejía, Copper(II) mixed chelate compounds induce apoptosis through reactive oxygen species in neuroblastoma cell line CHP-212, J. Inorg. Biochem. 126 (2013) 17–25, https://doi.org/10.1016/j.jinorgbio.2013.05.001.

[16] P.J. Cox, D. Kechagias, O. Kelly, Conformations of substituted benzophenones, Acta Crystallogr.. Sect. B. 64 (2008) 206–216, https://doi.org/10.1107/S0108768108000232.

[17] T.J. Boyle, L.A.M. Ottley, Structural characterization of the coordination behavior of 4,4′-di-methoxy,2,2′-di-ol-benzophenone modified metal alkoxides, Inorg. Chim. Acta. 364 (2010) 69–80, https://doi.org/10.1016/j.ica.2010.08.047.

[18] E. Mrkalić, A. Zianna, G. Psomas, M. Gdaniec, A. Czapik, E. Coutouli-Argyropoulou, M. Lalia-Kantouri, Synthesis, characterization, thermal and DNA-binding properties of new zinc complexes with 2-hydroxyphenones, J. Inorg. Biochem. 134 (2014) 66–75, https://doi.org/10.1016/j.jinorgbio.2014.01.019.

[19] E. Chiyindiko, E.H.G. Langner, J. Conradie, Electrochemical behaviour of copper (II) complexes containing 2-hydroxyphenones, Electrochim. Acta. 424 (2022), 140629, https://doi.org/10.1016/j.electacta.2022.140629.

[20] M. Enamullah, M. Anwar Hossain, M.K. Islam, D. Woschko, C. Janiak, Pseudotetrahedral copper(II)-complexes with enantiopure (R or S)-2-(((aryl)ethylimino)ethyl)phenolate Schiff base ligands, Dalton Trans.. 50 (2021) 9236–9249, https://doi.org/10.1039/D1DT01671G.

[21] A. Dehno Khalaji, M. Ghorbani, M. Dusek, V. Eigner, The Bis(4-methoxy-2-hydroxybenzophenone) copper(II) Complex Used as a New Precursor for Preparation of CuO Nanoparticles, Chem.. Methodol. 4 (2020) 143–151, https://doi.org/10.33945/SAMI/CHEMM.2020.2.4.

[22] C.B. Gonçalves, M.V. Marinho, D.F. Dias, M.H. Dos Santos, F.T. Martins, A. C. Doriguetto, Synthesis, characterization, and structural determination of copper (II) complexes with alkyl derivatives of hydroxybenzophenones, J. Coord. Chem. 70 (2017) 898–913, https://doi.org/10.1080/00958972.2017.1280783.

[23] M. Lashanizadegan, R.K. Alavijeh, M. Anafcheh, Facile synthesis of Co(II) and Cu (II) complexes of 2-hydroxybenzophenone: An efficient catalyst for oxidation of olefins and DFT study, J. Mol. Struct. 1146 (2017) 450–457, https://doi.org/10.1016/j.molstruc.2017.06.031.

[24] G.M. Sheldrick, Crystal structure refinement with SHELXL, Acta Crystallogr.. C Struct Chem. 71 (2015) 3–8, https://doi.org/10.1107/S2053229614024218.

[25] C.F. Macrae, I. Sovago, S.J. Cottrell, P.T.A. Galek, P. McCabe, E. Pidcock, M. Platings, G.P. Shields, J.S. Stevens, M. Towler, P.A. Wood, Mercury 4.0: from visualization to analysis, design and prediction, J. Appl. Cryst. 53 (2020) 226–235, https://doi.org/10.1107/S1600576719014092.

[26] S. Ansar Ahmed, R.M. Gogal, J.E. Walsh, A new rapid and simple non-radioactive assay to monitor and determine the proliferation of lymphocytes: an alternative to [3H]thymidine incorporation assay, J. Immunol. Methods. 170 (1994) 211–224, https://doi.org/10.1016/0022-1759(94)90396-4.

[27] A. Wolfe, G.H. Shimer, T. Meehan, Polycyclic aromatic hydrocarbons physically intercalate into duplex regions of denatured DNA, Biochemistry 26 (1987) 6392–6396, https://doi.org/10.1021/bi00394a013.

[28] J.R. Lakowicz, Principles of Fluorescence Spectroscopy, (2006).

[29] W.J. Geary, The use of conductivity measurements in organic solvents for the characterisation of coordination compounds, Coord. Chem. Rev. 7 (1971) 81–122, https://doi.org/10.1016/S0010-8545(00)80009-0.

[30] B.W. Liebich, E. Parthé, 2-Hydroxy-4-methoxybenzophenone, Acta Crystallogr.. Sect. B. 30 (1974) 2522–2524, https://doi.org/10.1107/S0567740874007503.

[31] H.L. Vasconcelos, T.P. Camargo, N.S. Gonçalves, A. Neves, M.C.M. Laranjeira, V. T. Fávere, Chitosan crosslinked with a metal complexing agent: Synthesis, characterization and copper(II) ions adsorption, React. Funct. Polym. 68 (2008) 572–579, https://doi.org/10.1016/j.reactfunctpolym.2007.10.024.

[32] C.O. D'Sousa, J.H. Araujo, I.R.S. Baliza, R.B. Dias, F. Valverde, M.T.A. Vidal, C.B. S. Sales, C.A.G. Rocha, D.R.M. Moreira, M.B.P. Soares, A.A. Batista, D.P. Bezerra, Novel piplartine-containing ruthenium complexes: synthesis, cell growth inhibition, apoptosis induction and ROS production on HCT116 cells, Oncotarget 8 (2017) 104367–104392, https://doi.org/10.18632/oncotarget.22248.

[33] G.R. Gonçalves, A.B. de Carvalho, J. Honorato, K.M. Oliveira, R.S. Correa, A new polymorph of six-coordinated bis(5,5′-dimethyl-2,2′-bipyridine) nitratocopper(II) nitrate and its DNA interactions, J. Mol. Struct. 1224 (2021), 129035, https://doi.org/10.1016/j.molstruc.2020.129035.

[34] J. do C. Almeida, R.T.C. Silva, R.D. Zanetti, M.B. Moreira, M.C. Portes, L. Polloni, F. V.P. de Vasconcelos Azevedo, G. Von Poelhsitz, M. Pivatto, A.V.G. Netto, V. de M. R. Ávila, K.F. Manieri, F.R. Pavan, A.M. Da Costa Ferreira, W. Guerra, DNA interactions, antitubercular and cytotoxic activity of heteroleptic CuII complexes containing 1,10-phenanthroline, J. Mol. Struct. 1235 (2021), https://doi.org/10.1016/j.molstruc.2021.130234, 130234.

[35] Y. Figueroa-DePaz, K. Resendiz-Acevedo, S.G. Dávila-Manzanilla, J.C. García-Ramos, L. Ortiz-Frade, J. Serment-Guerrero, L. Ruiz-Azuara, DNA, a target of mixed chelate copper(II) compounds (Casiopeinas®) studied by electrophoresis, UV–vis and circular dichroism techniques, J. Inorg. Biochem. 231 (2022), https://doi.org/10.1016/j.jinorgbio.2022.111772.

[36] J.P. Barolli, R.S. Correa, F.S. Miranda, J.U. Ribeiro, C. Bloch Jr., J. Ellena, V. Moreno, M.R. Cominetti, A.A. Batista, Polypyridyl ruthenium complexes: novel DNA-intercalating agents against human breast tumor, J. Braz. Chem. Soc. 28 (2017) 1879–1889.

[37] D.L. Boger, W.C. Tse, Thiazole orange as the fluorescent intercalator in a high resolution fid assay for determining DNA binding affinity and sequence selectivity of small molecules, Bioorg. Med. Chem. 9 (2001) 2511–2518, https://doi.org/10.1016/S0968-0896(01)00243-7.

[38] A. Kellett, Z. Molphy, C. Slator, V. McKee, N.P. Farrell, Molecular methods for assessment of non-covalent metallodrug–DNA interactions, Chem. Soc. Rev. 48 (2019) 971–988, https://doi.org/10.1039/C8CS00157J.

[39] S.U. Rehman, T. Sarwar, M.A. Husain, H.M. Ishqi, M. Tabish, Studying non-covalent drug–DNA interactions, Arch. Biochem.. Biophys. 576 (2015) 49–60, https://doi.org/10.1016/j.abb.2015.03.024.

[40] L. Yu, Z. Hua, X. Luo, T. Zhao, Y. Liu, Systematic interaction of plasma albumin with the efficacy of chemotherapeutic drugs, Biochim. Biophys. Acta (BBA) – Rev. Cancer 1877 (2022), 188655, https://doi.org/10.1016/j.bbcan.2021.188655.
[41] M. Ganeshpandian, R. Loganathan, E. Suresh, A. Riyasdeen, M.A. Akbarsha, M. Palaniandavar, New ruthenium(ii) arene complexes of anthracenyl-appended diazacycloalkanes: effect of ligand intercalation and hydrophobicity on DNA and protein binding and cleavage and cytotoxicity, Dalton Trans. 43 (2014) 1203–1219, https://doi.org/10.1039/c3dt51641e.
[42] K.M. Oliveira, J. Honorato, F.C. Demidoff, M.S. Schultz, C.D. Netto, M. R. Cominetti, R.S. Correa, A.A. Batista, Lapachol in the design of a new ruthenium (II)-diphosphine complex as a promising anticancer metallodrug, J. Inorg. Biochem. 214 (2021), 111289, https://doi.org/10.1016/j.jinorgbio.2020.111289.